Theoretical study of scalar meson $a_0(1710)$ in the $\eta_c \to \bar{K}^0 K^+ \pi^-$ reaction

Yan Ding[1], Xiao-Hui Zhang,[1] Meng-Yuan Dai,[1] En Wang[1,2,*]
De-Min Li,[1,†] Li-Sheng Geng,[3,4,5,6,‡] and Ju-Jun Xie[7,8,6,§]

[1]*School of Physics and Microelectronics, Zhengzhou University, Zhengzhou, Henan 450001, China*
[2]*Guangxi Key Laboratory of Nuclear Physics and Nuclear Technology,*
Guangxi Normal University, Guilin 541004, China
[3]*School of Physics, Beihang University, Beijing 102206, China*
[4]*Beijing Key Laboratory of Advanced Nuclear Materials and Physics,*
Beihang University, Beijing 102206, China
[5]*Peng Huanwu Collaborative Center for Research and Education,*
Beihang University, Beijing 100191, China
[6]*Southern Center for Nuclear-Science Theory (SCNT), Institute of Modern Physics,*
Chinese Academy of Sciences, Huizhou 516000, China
[7]*Institute of Modern Physics, Chinese Academy of Sciences, Lanzhou 730000, China*
[8]*School of Nuclear Sciences and Technology,*
University of Chinese Academy of Sciences, Beijing 101408, China

We investigate the process $\eta_c \to \bar{K}^0 K^+ \pi^-$ by taking into account the S-wave $K^* \bar{K}^*$ and $\rho\omega$ interactions within the unitary coupled-channel approach, where the scalar meson $a_0(1710)$ is dynamically generated. In addition, the contributions from the intermediate resonances $K_0^*(1430)^- \to \bar{K}^0 \pi^-$ and $K_0^*(1430)^0 \to K^+ \pi^-$ are also considered. We find a significant dip structure around 1.8 GeV, associated to the $a_0(1710)$, in the $\bar{K}^0 K^+$ invariant mass distribution, and the clear peaks of the $K_0^*(1430)$ in the $\bar{K}^0 \pi^-$ and $K^+ \pi^-$ invariant mass distributions, consistent with the *BABAR* measurements. We further estimate the branching fractions $\mathcal{B}(\eta_c \to \bar{K}^{*0} K^{*+} \pi^-) = 5.5 \times 10^{-3}$ and $\mathcal{B}(\eta_c \to \omega\rho^+\pi^-) = 7.9 \times 10^{-3}$. Our predictions can be tested by the BESIII and Belle II experiments in the future.

I. INTRODUCTION

In 2021, the *BABAR* Collaboration observed the scalar resonance $a_0(1710)$ in the $\pi^{\pm}\eta$ invariant mass spectrum of the process $\eta_c \to \eta\pi^+\pi^-$ [1]. In 2022, the BESIII Collaboration also found the $a_0(1710)$ state in the $K_S^0 K_S^0$ invariant mass spectrum of the process $D_s^+ \to K_S^0 K_S^0 \pi^+$ [2], and in the $K_S^0 K^+$ invariant mass spectrum of the process $D_s^+ \to K_S^0 K^+ \pi^0$ [3]. The experimental measurements of the mass and width of $a_0(1710)$ are tabulated in Table I. One can see that there are some discrepancies between the measured masses. Note that in Ref. [2], BESIII did not distinguish between the $a_0(1710)$ and $f_0(1710)$ in the

process $D_s^+ \to K_S^0 K_S^0 \pi^+$, and denoted the combined state as $S(1710)$, while in Ref. [3] the $a_0(1710)$ was renamed as $a_0(1817)$ because of the different fitted mass of this state.

It should be stressed that there have been many theoretical studies about the structure of the $a_0(1710)$ and its isospin partner $f_0(1710)$ from various perspectives [4–16]. For the $f_0(1710)$, although it is a well-established state according to the Review of Particle Physics (RPP) [17], there are still different interpretations of its structure. In Ref. [12], it was shown that the $f_0(1710)$ wave function contains a large $s\bar{s}$ component, while in Refs. [13–16], it was regarded as a scalar glueball. In addition, the $f_0(1710)$ and $a_0(1710)$ states could be dynamically generated from the vector-vector interactions [18,19], and this picture remains essentially the same when the pseudoscalar-pseudoscalar coupled-channels were taken into account [20]. In Ref. [21], one isovector scalar state a_0 with a mass of 1744 MeV is also predicted in the approach of Regge trajectories, which is roughly consistent with the experimental mass of the $a_0(1710)$.

As shown in Table I, the mass of the $a_0(1710)$ is not well determined experimentally. This can complicate the understanding of the nature of the $a_0(1710)$. For instance,

*wangen@zzu.edu.cn
†lidm@zzu.edu.cn
‡lisheng.geng@buaa.edu.cn
§xiejujun@impcas.ac.cn

TABLE I. Experimental measurements on the mass and width of the scalar state $a_0(1710)$. The first error is statistical and the second one is systematic. All values are in units of MeV.

Experiment	$M_{a_0(1710)}$	$\Gamma_{a_0(1710)}$	Reference
BABAR	$1704 \pm 5 \pm 2$	$110 \pm 15 \pm 11$	[1]
BESIII	$1723 \pm 11 \pm 2$	$140 \pm 14 \pm 4$	[2]
BESIII	$1817 \pm 8 \pm 20$	$97 \pm 22 \pm 15$	[3]

$a_0(1710)$ [or $a_0(1817)$] and $X(1812)$ have been explained as the 3^3P_0 state by assuming $a_0(980)$ and $f_0(980)$ as 1^3P_0 states [22]. Indeed, $X(1812)$ was observed in the process $J/\psi \to \gamma\phi\omega$ by the BESIII Collaboration [23,24], and the enhancement near the $\phi\omega$ threshold, associated to $X(1812)$, could be described by the reflection of $f_0(1710)$, as discussed in Ref. [8]. By regarding the $a_0(1710)$ as a $K^*\bar{K}^*$ molecular state, Refs. [25–29] have successfully described the invariant mass distributions of the processes $D_s^+ \to K_S^0 K_S^0 \pi^+$ and $D_s^+ \to K_S^0 K^+ \pi^0$ measured by the BESIII Collaboration.

Since the peak positions of the $a_0(1710)$ in the $K\bar{K}$ invariant mass distributions of the processes $D_s^+ \to K_S^0 K_S^0 \pi^+, K_S^0 K^+ \pi^0$ observed by the BESIII Collaboration are very close to the boundary region of the $K\bar{K}$ invariant mass, it is crucial to measure the properties of the $a_0(1710)$ precisely in other processes with larger phase space [30]. Taking into account that the dominant decay channel of the $a_0(1710)$ is $K\bar{K}$ in the molecular picture [18,20], we propose to search for this state in the process $\eta_c \to \bar{K}^0 K^+ \pi^-$. Indeed, there have been some experimental studies of this process. In 2012, the BESIII Collaboration has measured the branching fraction $\mathcal{B}(\eta_c \to K_S^0 K^\pm \pi^\mp) = (2.60 \pm 0.29 \pm 0.34 \pm 0.25)\%$ via $\psi(3686) \to \pi^0 h_c, h_c \to \gamma\eta_c$ with a sample of 106 million $\psi(3686)$ events [31]. In 2019, the BESIII Collaboration measured the branching fraction of this process $\mathcal{B}(\eta_c \to K_S^0 K^\pm \pi^\mp) = (2.60 \pm 0.21 \pm 0.20)\%$ via $e^+ e^- \to \pi^+ \pi^- h_c, h_c \to \gamma\eta_c$ with the data samples collected at $\sqrt{s} = 4.23$, 4.26, 4.36, and 4.42 GeV [32]. In addition, the *BABAR* Collaboration has observed this process in the $\gamma\gamma^* \to \eta_c \to K_S^0 K^\pm \pi^\mp$ [33,34], and the measured $K_S^0 K^+$ mass spectrum shows some structure in the region of 1.7–1.8 GeV, which could hint at the existence of the $a_0(1710)$, as we show in this work.

Based on the *BABAR* data [33,34], we will investigate the process $\eta_c \to \bar{K}^0 K^+ \pi^-$. In addition to the contribution from the scalar resonance $a_0(1710)$, we also take into account the contribution from the intermediate resonance $K_0^*(1430)$, which plays an important role in this process according to Refs. [33,34].

The paper is organized as follows. In Sec. II, we present the theoretical formalism of the $\eta_c \to \bar{K}^0 K^+ \pi^-$ decay, and in Sec. III, we show our numerical results and discussions, followed by a short summary in the last section.

II. FORMALISM

First in Sec. II A we present the theoretical formalism for the process $\eta_c \to \bar{K}^0 K^+ \pi^-$ via the $K^*\bar{K}^*$ and $\omega\rho$ final state interactions, which dynamically generate the scalar resonance $a_0(1710)$. Next, we show the formalism for the process $\eta_c \to K_0^*(1430)^- K^+ [K_0^*(1430)^0 \bar{K}^0]$ with $K_0^*(1430)^- \to K^0\pi^-$ $[K_0^*(1430)^0 \to K^+\pi^-]$ in Sec. II B. Finally, the formalism for the double differential widths of the process $\eta_c \to \bar{K}^0 K^+ \pi^-$ is given in Sec. II C.

A. Mechanism of $\eta_c \to (\bar{K}^{*0} K^{*+}/\omega\rho^+)\pi^- \to \bar{K}^0 K^+ \pi^-$

With the assumption that the η_c is a singlet of SU(3), and $a_0(1710)$ is a vector-vector molecular state [18,19], one needs to first produce the vector-vector pairs in the η_c decay. Considering that this process has a π^- in the final states, we introduce one combination mode of $\langle VVP \rangle$ in the primary vertex [35,36], where V and P are the SU(3) vector and pseudoscalar matrices respectively [35–39],

$$V = \begin{pmatrix} \frac{\rho^0}{\sqrt{2}} + \frac{\omega}{\sqrt{2}} & \rho^+ & K^{*+} \\ \rho^- & -\frac{\rho^0}{\sqrt{2}} + \frac{\omega}{\sqrt{2}} & K^{*0} \\ K^{*-} & \bar{K}^{*0} & \phi \end{pmatrix}, \quad (1)$$

$$P = \begin{pmatrix} \frac{\eta}{\sqrt{3}} + \frac{\pi^0}{\sqrt{2}} + \frac{\eta'}{\sqrt{6}} & \pi^+ & K^+ \\ \pi^- & \frac{\eta}{\sqrt{3}} - \frac{\pi^0}{\sqrt{2}} + \frac{\eta'}{\sqrt{6}} & K^0 \\ K^- & \bar{K}^0 & -\frac{\eta}{\sqrt{3}} + \frac{\sqrt{6}\eta'}{3} \end{pmatrix}, \quad (2)$$

where the $\eta - \eta'$ mixing is assumed according to Ref. [40]. The symbol $\langle \rangle$ stands for the trace of the SU(3) matrices. One could obtain the relevant contributions by isolating the terms containing π^-, as follows,

$$\langle VVP \rangle$$
$$= (VV)_{12} P_{21}$$
$$= \pi^- \sum_i V_{1i} V_{i2}$$
$$= \pi^- \left[\rho^+ \left(\frac{\rho^0}{\sqrt{2}} + \frac{\omega}{\sqrt{2}} \right) + \left(-\frac{\rho^0}{\sqrt{2}} + \frac{\omega}{\sqrt{2}} \right) \rho^+ + \bar{K}^{*0} K^{*+} \right]$$
$$= \pi^- [\sqrt{2}\rho^+ \omega + \bar{K}^{*0} K^{*+}]. \quad (3)$$

In the molecular picture, the $a_0(1710)$ is dynamically generated from the S-wave $\bar{K}^{*0} K^{*+}$ and $\omega\rho^+$ final-state interactions [18,19], and then decays into the final states $\bar{K}^0 K^+$, as depicted in Fig. 1. The decay amplitude of Fig. 1 can be written as,
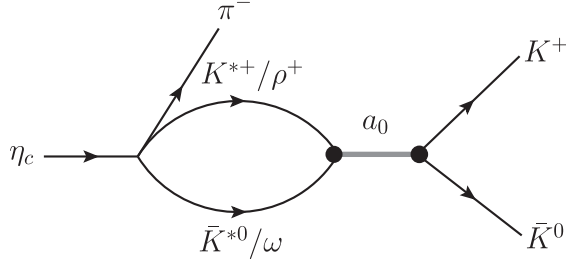
FIG. 1. Diagram for the process $\eta_c \to (\bar{K}^{*0}K^{*+}/\omega\rho^+)\pi^- \to a_0(1710)^+\pi^- \to \bar{K}^0K^+\pi^-$.

$$\mathcal{M}_a = V_p \times (G_{\bar{K}^{*0}K^{*+}}t_{\bar{K}^{*0}K^{*+}\to\bar{K}^0K^+} \\ + \sqrt{2}G_{\omega\rho^+}t_{\omega\rho^+\to\bar{K}^0K^+}), \qquad (4)$$

where V_P is the normalization factor, and $t_{\bar{K}^{*0}K^{*+}\to\bar{K}^0K^+}$ and $t_{\omega\rho^+\to\bar{K}^0K^+}$ are the transition amplitudes.

The loop functions $G_{\bar{K}^{*0}K^{*+}}$ and $G_{\omega\rho^+}$ are for the $\bar{K}^{*0}K^{*+}$ and $\omega\rho^+$ channels, respectively, and read [18,41],

$$G_i(M_{\bar{K}^0K^+}) = \int_{m_{1-}^2}^{m_{1+}^2} \int_{m_{2-}^2}^{m_{2+}^2} d\tilde{m}_1^2 d\tilde{m}_2^2 \\ \times \omega(\tilde{m}_1^2)\omega(\tilde{m}_2^2)\tilde{G}(M_{\bar{K}^0K^+},\tilde{m}_1^2,\tilde{m}_2^2), \quad (5)$$

where

$$\omega(\tilde{m}_i^2) = \frac{1}{N}\text{Im}\left[\frac{1}{\tilde{m}_i^2 - m_{V_i}^2 + i\Gamma(\tilde{m}_i^2)\tilde{m}_i}\right], \qquad (6)$$

$$N = \int_{\tilde{m}_{i-}^2}^{\tilde{m}_{i+}^2} d\tilde{m}_i^2 \text{Im}\left[\frac{1}{\tilde{m}_i^2 - m_{V_i}^2 + i\Gamma(\tilde{m}_i^2)\tilde{m}_i}\right], \qquad (7)$$

$$\Gamma(\tilde{m}_i^2) = \Gamma_{V_i}\frac{\tilde{k}^3}{k^3}, \qquad (8)$$

$$\tilde{k} = \frac{\lambda^{\frac{1}{2}}(\tilde{m}_i^2, m_{P_1}^2, m_{P_2}^2)}{2\tilde{m}_i}, \quad k = \frac{\lambda^{\frac{1}{2}}(m_{V_i}^2, m_{P_1}^2, m_{P_2}^2)}{2m_{V_i}}, \quad (9)$$

with the Källen function $\lambda(x,y,z) = x^2 + y^2 + z^2 - 2xy - 2xz - 2yz$. Here, we consider the decay channels $\pi\pi$ and $K\pi$ for the vector mesons ρ and K^*, respectively, and neglect the contribution from the small width ($\Gamma_\omega = 8.68$ MeV) of ω. Taking the vector K^* for example, $m_{1+}^2 = (m_{K^*} + 2\Gamma_{K^*})^2$ and $m_{1-}^2 = (m_{K^*} - 2\Gamma_{K^*})^2$. Similarly, one can obtain m_{1+}^2 and m_{1-}^2 for the ρ. The masses, widths, and spin-parities of the involved particles are taken from the RPP [17], and listed in Table II.

The loop function $\tilde{G}$ of Eq. (5) is for stable particles, and in the dimensional regularization scheme it can be written as [18],

TABLE II. Masses, widths, and spin-parities of the involved particles in this work. All values are in units of MeV.

Particle	Mass	Width	Spin-parity (J^P)
η_c	2983.9	32.0	0^-
$\pi^\pm$	139.5704	$\cdots$	0^-
$\bar{K}^0$	497.611	$\cdots$	0^-
$K^\pm$	493.677	$\cdots$	0^-
K^*	893.6	49.1	1^-
ω	782.65	8.68	1^-
ρ	775.26	149.1	1^-
$K_0^*(1430)$	1425	270	0^+

$$\tilde{G} = \frac{1}{16\pi^2}\left\{a_\mu + \ln\frac{m_1^2}{\mu^2} + \frac{m_2^2 - m_1^2 + s}{2s}\ln\frac{m_2^2}{m_1^2}\right. \\ \times\frac{p}{\sqrt{s}}\left[\ln(s - (m_2^2 - m_1^2) + 2p\sqrt{s})\right. \\ + \ln(s + (m_2^2 - m_1^2) + 2p\sqrt{s}) \\ - \ln(-s + (m_2^2 - m_1^2) + 2p\sqrt{s}) \\ \left.\left. - \ln(-s - (m_2^2 - m_1^2) + 2p\sqrt{s})\right]\right\}, \qquad (10)$$

with

$$p = \frac{\lambda^{1/2}(s, m_1^2, m_2^2)}{2\sqrt{s}}, \qquad (11)$$

where a_μ is the subtraction constant, μ is the dimensional regularization scale, and $s = M_{\bar{K}^0K^+}^2$. We take $a_\mu = -1.726$ and $\mu = 1000$ MeV as used in Ref. [18]. It is worth mentioning that any change in μ could be reabsorbed by a change in a_μ through $a_{\mu'} - a_\mu = \ln(\mu'^2/\mu^2)$, which implies that the loop function $\tilde{G}$ is scale independent [42].

In order to show the influence of the widths of vector mesons on the loop functions, we calculate the loop function $G_{\omega\rho}$ and $\tilde{G}_{\omega\rho}$ as functions of the $\bar{K}^0K^+$ invariant mass, and show them in Fig. 2. The blue long-dashed and red dot-dashed curves correspond to the real and imaginary parts of the loop function G considering the width of ρ, respectively. While, the green solid and purple dotted curves correspond to the real and imaginary parts of the loop function $\tilde{G}$ without the contribution from the ρ width, respectively. One can see that the loop function G, considering the width of the vector meson, becomes smoother around the threshold.

On the other hand, the transition amplitudes $t_{\bar{K}^{*0}K^{*+}/\omega\rho^+\to\bar{K}^0K^+}$ in Eq. (4) could be obtained from the coupled-channel approach in Ref. [10], where one state a_0 with mass around 1760 MeV could be dynamically generated from the $\eta\pi$, $\bar{K}K$, $\omega\rho$, $\phi\rho$, and $\bar{K}^*K^*$ interactions within SU(6) spin-flavor symmetry. However, the width of a_0 is about 24 MeV, much smaller than the one for the
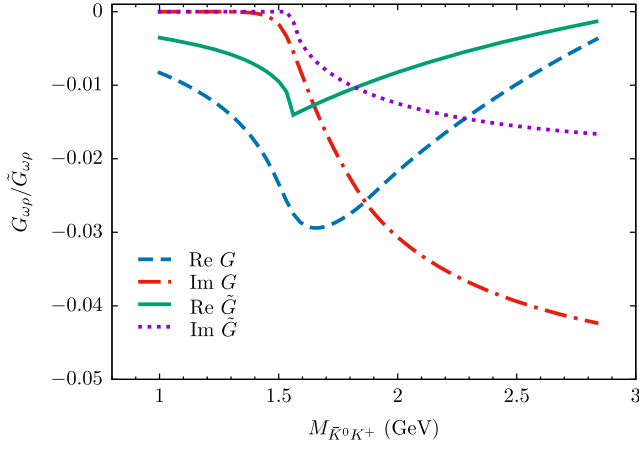
FIG. 2. Real and imaginary parts of the loop functions $G_{\omega\rho}$ and $\tilde{G}_{\omega\rho}$ as a function of the $\bar{K}^0 K^+$ invariant mass.

$a_0(1710)$ resonance as quoted in the PDG [17]. On the other hand, it is customary to obtain the coupling constants and the pole position of the dynamically generated state by fitting the Breit-Wigner form to the amplitude of the coupled-channel approach around the pole position,

$$T_{ij} = \frac{g_i g_j}{s - s_{\text{pole}}}, \tag{12}$$

where $g_{i(j)}$ is the couplings to channel i (j). It implies that the amplitude of the Breit-Wigner form with the same position and couplings should give similar behavior around the pole position. Thus, we take the transition amplitude as,

$$t_{\bar{K}^0 K^{*+}/\omega\rho^+ \to \bar{K}^0 K^+} = \frac{g_{K^*\bar{K}^*/\omega\rho} \times g_{K\bar{K}}}{M^2_{\bar{K}^0 K^+} - M^2_{a_0} + iM_{a_0}\Gamma_{a_0}}, \tag{13}$$

where M_{a_0} and Γ_{a_0} are the mass and width of the $a_0(1710)$, respectively, and we take their values from Refs. [18,43], which are tabulated in Table III. $g_{K^*\bar{K}^*}$, $g_{\omega\rho}$, and $g_{K\bar{K}}$ are the coupling constants of the vertices $K^*\bar{K}^*/\omega\rho \to a_0(1710)^1$ and $a_0(1710) \to K\bar{K}$, respectively, whose values are determined in Ref. [18]. We determine the coupling $g_{K\bar{K}}$ from the partial decay width of $a_0(1710) \to K\bar{K}$,

$$\Gamma_{K\bar{K}} = \frac{g^2_{K\bar{K}}}{8\pi} \frac{|\vec{p}_K|}{M^2_{a_0}}, \tag{14}$$

where $\vec{p}_K$ is the three momentum of the K or $\bar{K}$ meson in the $a_0(1710)$ rest frame,

---

[1]The couplings of $a_0(1710)$ to the channels $K^*\bar{K}^*$ and $\omega\rho$ are obtained at the pole position [18]. In this work, we take the coupling to be complex, and do not consider the extra phase interference between the coupled-channels $K^*\bar{K}^*$ and $\omega\rho$.

TABLE III. Mass, width, and coupling constants of the scalar $a_0(1710)$ [18]. $g_{K^*\bar{K}^*}$, $g_{\omega\rho}$, and $g_{K\bar{K}}$ stand for the coupling constants of $a_0(1710)$ to the $K^*\bar{K}^*$, $\omega\rho$, and $K\bar{K}$ channels, respectively, while $\Gamma_{K\bar{K}}$ denotes the partial decay width of the $a_0(1710) \to K\bar{K}$. All values are in units of MeV.

Parameters	Value
M_{a_0}	1777
Γ_{a_0}	148.0
$g_{K^*\bar{K}^*}$	$(7525, -i1529)$
$g_{\omega\rho}$	$(-4042, i1393)$
$g_{K\bar{K}}$	1966
$\Gamma_{K\bar{K}}$	36

$$|\vec{p}_K| = \frac{\lambda^{1/2}(M^2_{a_0}, m^2_{\bar{K}}, m^2_K)}{2M_{a_0}}. \tag{15}$$

With the partial decay width $\Gamma_{K\bar{K}} = 36$ MeV [18], one can only obtain the absolute value of the coupling constant, but not the phase, thus we assume that $g_{K\bar{K}}$ is real and positive in this work, as done in Refs. [25,26].

B. Mechanism of $\eta_c \to (K^+ K_0^*(1430)^-/\bar{K}^0 K_0^*(1430)^0) \to \bar{K}^0 K^+ \pi^-$

First, we show the diagram for the process $\eta_c \to K^+ K_0^*(1430)^-$, followed by the decay $K_0^*(1430)^- \to \bar{K}^0 \pi^-$ in S-wave, in Fig. 3.

The decay amplitude for $\eta_c \to K^+ K_0^*(1430)^- \to \bar{K}^0 K^+ \pi^-$ of Fig. 3 can be written as

$$\mathcal{M}_b = \frac{g_{\eta_c K^+ K_0^{*-}} g_{K_0^{*-}\bar{K}^0 \pi^-}}{M^2_{\bar{K}^0 \pi^-} - M^2_{K_0^*} + iM_{K_0^*}\Gamma_{K_0^*}}, \tag{16}$$

where $M_{\bar{K}^0 \pi^-}$ is the invariant mass of the $\bar{K}^0 \pi^-$ system, and $g_{\eta_c K^+ K_0^{*-}}$ and $g_{K_0^{*-}\bar{K}^0 \pi^-}$ denote the coupling constants of $\eta_c \to K^+ K_0^{*-}$ and $K_0^{*-} \to \bar{K}^0 \pi^-$, respectively. The mass and width of the $K_0^*(1430)$ are given in Table II.

Similarly, as shown in Fig. 4, the amplitude of the process $\eta_c \to \bar{K}^0 K_0^*(1430)^0 \to \bar{K}^0 K^+ \pi^-$ can be expressed as,

$$\mathcal{M}_c = \frac{g_{\eta_c \bar{K}^0 K_0^{*0}} g_{K_0^{*0} K^+ \pi^-}}{M^2_{K^+ \pi^-} - M^2_{K_0^*} + iM_{K_0^*}\Gamma_{K_0^*}}, \tag{17}$$
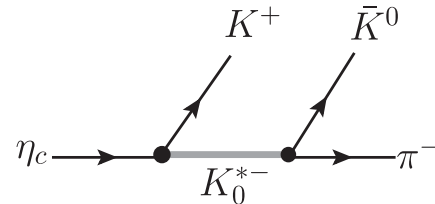
FIG. 3. Diagram for $\eta_c \to \bar{K}^0 K^+ \pi^-$ via the intermediate $K_0^*(1430)^-$, followed by the decay $K_0^*(1430)^- \to \bar{K}^0 \pi^-$.
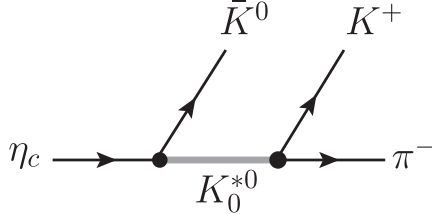
FIG. 4. Diagram for $\eta_c \to \bar{K}^0 K^+ \pi^-$ via the intermediate $K_0^*(1430)^0$, followed by the decay $K_0^*(1430)^0 \to K^+\pi^-$.

where $M_{K^+\pi^-}$ is the $K^+\pi^-$ invariant mass, and $g_{\eta_c \bar{K}^0 K_0^{*0}}$ and $g_{K_0^{*0} K^+\pi^-}$ are the coupling constants of the vertices $\eta_c \to \bar{K}^0 K_0^*(1430)^0$ and $K_0^*(1430)^0 \to K^+\pi^-$, respectively.

The coupling constants appearing in Eqs. (16) and (17) could be determined from the experimental partial decay widths of $\eta_c \to KK_0^*(1430)$ and $K_0^*(1430) \to \bar{K}\pi$, respectively. The effective Lagrangians accounting for the vertices of $\eta_c \to KK_0^*(1430)$ and $K_0^*(1430) \to K\pi$ are given by [44],

$$\mathcal{L} = g_{\eta_c KK_0^*} \eta_c KK_0^* \tag{18}$$

$$\mathcal{L} = g_{K_0^* K\pi} K_0^* K\pi. \tag{19}$$

With the above effective Lagrangians, we can express the corresponding partial decay widths as,

$$\Gamma_{\eta_c \to K_0^* K} = \frac{g_{\eta_c K_0^* K}^2}{8\pi} \frac{|\mathbf{P}|}{m_{\eta_c}^2}, \tag{20}$$

$$\Gamma_{K_0^* \to K\pi} = \frac{g_{K_0^* K\pi}^2}{8\pi} \frac{|\mathbf{P}|}{m_{K_0^*}^2}, \tag{21}$$

where $\mathbf{P}$ is the three-momentum of the two final-state particles in the rest frame of the parent particle, which reads,

$$|\mathbf{P}| = \frac{\lambda^{1/2}(M^2, m_1^2, m_2^2)}{2M}, \tag{22}$$

and M and $m_{1,2}$ are the masses of the initial parent particle and the two final-state mesons, respectively. The masses and widths of these particles are given in Table II.

According to the RPP [17], the branching fraction of $K_0^* \to K\pi$ is $\mathcal{B}(K_0^* \to K\pi) = (93 \pm 10)\%$, and we take it to be 100% in this work. One can then easily obtain the coupling constant $g_{K_0^* K\pi} = 4721$ MeV.

In addition, with the branching fraction $\mathcal{B}(\eta_c \to \bar{K}^0 K^+ \pi^-) = (2.4 \pm 0.2)\%$ [45] and the ratio of $\mathcal{B}(\eta_c \to K_0^{*0} \bar{K}^0 / K_0^{*-} K^+)/\mathcal{B}(\eta_c \to \bar{K}^0 K^+ \pi^-) = (40.8 \pm 2.2)\%$ [33], we could estimate the branching fraction $\mathcal{B}(\eta_c \to K_0^{*0} \bar{K}^0) = \mathcal{B}(\eta_c \to K_0^{*0} K^+) = (0.5 \pm 0.1)\%$. Then, we can determine the coupling constants $g_{\eta_c K^+ K_0^{*-}} = g_{\eta_c \bar{K}^0 K_0^{*0}} = 180$ MeV. It

TABLE IV. Coupling constants of the $K_0^*(1430)$.

Decay process	Fraction	Decay width (MeV)	Coupling constant	Value (MeV)
$\eta_c \to K^+ K_0^{*-}$	$(0.5 \pm 0.1)\%$	32.0 ± 0.7	$g_{\eta_c K^+ K_0^{*-}}$	180
$K_0^* \to K\pi$	$(93 \pm 10)\%$	270 ± 80	$g_{K_0^* K\pi}$	4721
$\eta_c \to \bar{K}^0 K_0^{*0}$	$(0.5 \pm 0.1)\%$	32.0 ± 0.7	$g_{\eta_c \bar{K}^0 K_0^{*0}}$	180

is worth mentioning that the coupling constants appearing in Eqs. (16) and (17) are assumed to be real and positive, and the values of those coupling constants are listed in Table IV.

C. Invariant mass distributions

With the amplitudes obtained above, we can write down the total decay amplitude of $\eta_c \to \bar{K}^0 K^+ \pi^-$ as follows,

$$\mathcal{M} = \mathcal{M}_a + \mathcal{M}_b + \mathcal{M}_c, \tag{23}$$

and the double differential widths of the process $\eta_c \to \bar{K}^0 K^+ \pi^-$ are

$$\frac{d^2\Gamma}{dM_{\bar{K}^0 K^+} dM_{K^+\pi^-}} = \frac{M_{\bar{K}^0 K^+} M_{K^+\pi^-}}{128\pi^3 m_{\eta_c}^3} |\mathcal{M}|^2, \tag{24}$$

$$\frac{d^2\Gamma}{dM_{\bar{K}^0 K^+} dM_{\bar{K}^0\pi^-}} = \frac{M_{\bar{K}^0 K^+} M_{\bar{K}^0\pi^-}}{128\pi^3 m_{\eta_c}^3} |\mathcal{M}|^2. \tag{25}$$

Furthermore, one can easily obtain $d\Gamma/dM_{\bar{K}^0 K^+}$, $d\Gamma/dM_{\bar{K}^0\pi^-}$, and $d\Gamma/dM_{K^+\pi^-}$ by integrating over each of the invariant mass variables with the limits of the Dalitz plot given in the RPP [17]. For example, the upper and lower limits for $M_{\bar{K}^0 K^+}$ are

$$(M_{\bar{K}^0 K^+}^2)_{\max} = (E_{K^+}^* + E_{\bar{K}^0}^*)^2$$
$$- \left(\sqrt{E_{K^+}^{*2} - m_{K^+}^2} - \sqrt{E_{\bar{K}^0}^{*2} - m_{\bar{K}^0}^2} \right)^2$$

$$(M_{\bar{K}^0 K^+}^2)_{\min} = (E_{K^+}^* + E_{\bar{K}^0}^*)^2$$
$$- \left(\sqrt{E_{K^+}^{*2} - m_{K^+}^2} + \sqrt{E_{\bar{K}^0}^{*2} - m_{\bar{K}^0}^2} \right)^2,$$

where $E_{K^+}^*$ and $E_{\bar{K}^0}^*$ are the energies of K^+ and $\bar{K}^0$ in the $\bar{K}^0\pi^-$ rest frame, respectively,

$$E_{\bar{K}^0}^* = \frac{M_{\bar{K}^0\pi^-}^2 - m_{\pi^-}^2 + m_{\bar{K}^0}^2}{2M_{\bar{K}^0\pi^-}},$$

$$E_{K^+}^* = \frac{m_{\eta_c}^2 - M_{\bar{K}^0\pi^-}^2 - m_{K^+}^2}{2M_{\bar{K}^0\pi^-}}. \tag{26}$$

III. RESULTS AND DISCUSSION

It should be pointed out that the $K_S^0 K^+$ invariant mass distribution of the process $\eta_c \to K_S^0 K^+ \pi^-$ has been
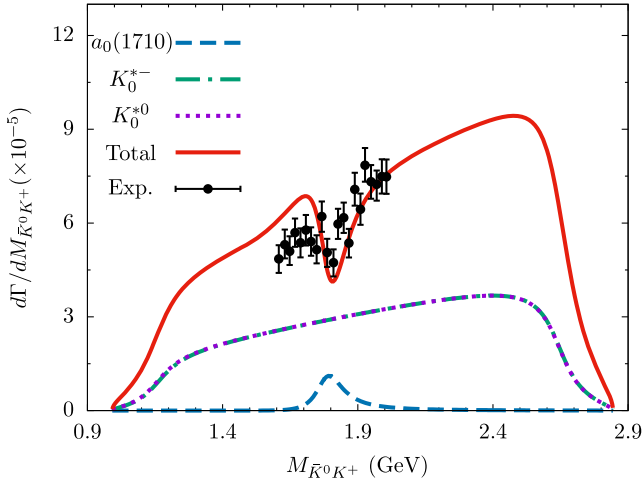
FIG. 5. $\bar{K}^0 K^+$ invariant mass distribution of the process $\eta_c \to \bar{K}^0 K^+ \pi^-$. The red-solid curve stands for the total contributions, while the blue-dashed curve, the green-dot-dashed curve, and purple-dotted curve correspond to the contribution from the $a_0(1710)$ state, the intermediate $K_0^*(1430)^-$, and $K_0^*(1430)^0$, respectively. The *BABAR* data are taken from Fig. 7(a) of Ref. [33].

FIG. 6. $\bar{K}^0 K^+$ invariant mass distribution of the process $\eta_c \to \bar{K}^0 K^+ \pi^-$ with the parameter $V_p = 0.6$, 0.8, 1.0, respectively. In addition to the *BABAR* measurements of the $\eta_c \to \bar{K}^0 K^+ \pi^-$ [33] (labeled as *BABAR* 2016), we also show the *BABAR* measurements of the $K^+ K^-$ invariant mass distribution of the process $\eta_c \to K^+ K^- \pi^0$ [46] (labeled as *BABAR* 2014).

measured by the *BABAR* Collaboration [33]. In this work, we take $V_p = 0.8$ in order to match with the *BABAR* measurements of the $K_S^0 K^+$ invariant mass distribution around 1.6–2.1 GeV. In Fig. 5, we show our results of the $\bar{K}^0 K^+$ invariant mass distribution, where the red-solid curve stands for the total contribution from the $a_0(1710)$ state and the vector K_0^* meson, while the blue-dashed curve corresponds to the contribution from the $a_0(1710)$ state. Moreover, the green-dot-dashed and purple-dotted curves stand for the contributions from the intermediate $K_0^*(1430)^-$ and $K_0^*(1430)^0$, respectively. We also show the *BABAR* data points in the region of 1.6–2.1 GeV,[2] which has been multiplied by an overall normalization factor 4×10^{-7} [33]. As one can see from Fig. 5, the contributions from the $K_0^*(1430)$ are smooth in the region of 1.4–2.4 GeV. In particular, we note that the dip structure around 1800 MeV is in agreement with the *BABAR* measurement [33]. This dip structure is mainly due to the interference between the contributions from the $a_0(1710)$ and the $K_0^*(1430)$, and should be associated to the scalar $a_0(1710)$.

In order to show the dependence of our results on the parameter V_p, we present the $\bar{K}^0 K^+$ invariant mass distribution of the process $\eta_c \to \bar{K}^0 K^+ \pi^-$ with the parameter $V_p = 0.6$, 0.8, 1.0 in Fig. 6. One can see that the dip structure around 1.8 GeV persists, which is in agreement

with the *BABAR* measurements [33], labeled as *BABAR* 2016. It should be stressed that the *BABAR* Collaboration has also measured the $K^+ K^-$ invariant mass distribution of the process $\eta_c \to K^+ K^- \pi^0$, as shown by the data of *BABAR* 2014 in Fig. 6, where one dip structure also appears around 1.8 GeV [46].

However, it should be pointed out that the dip structure appearing in the $\bar{K}^0 K^+$ invariant mass distribution of Fig. 5 could also manifest itself as a peak structure if the interference between $\mathcal{M}_a$, $\mathcal{M}_b$, and $\mathcal{M}_c$ are different from our naive assignments explained above. For instance, if we multiply the term $\mathcal{M}_a$ of Eq. (23) by a phase factor $e^{i\phi}$ with
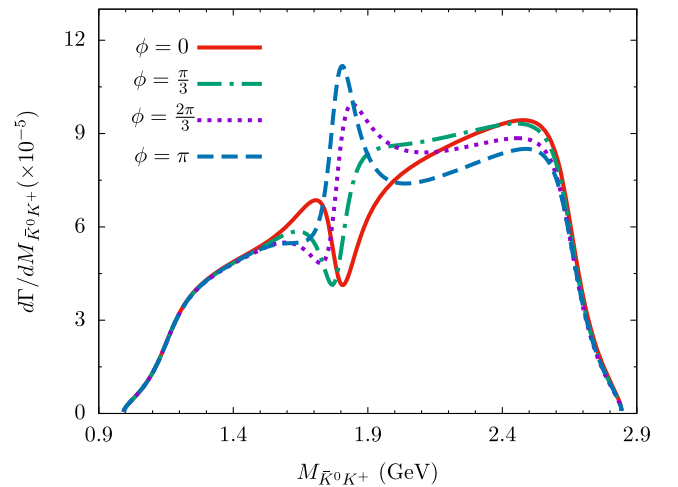
FIG. 7. $\bar{K}^0 K^+$ invariant mass distribution of the process $\eta_c \to \bar{K}^0 K^+ \pi^-$ obtained with a phase angle $\phi = 0$, $\pi/3$, $2\pi/3$, and π, respectively. See the text for details.

___

[2]As pointed out in Ref. [33], for the $\eta_c \to \bar{K}^0 K^+ \pi^-$ decay, some other resonances also contribute, such as the $a_0(980)$, $a_0(1450)$, $a_0(1950)$, and $a_2(1320)$. Since in this work we focus on the possible signal of the $a_0(1710)$, only the *BABAR* data in the region of 1.6–2.1 GeV are presented in Figs. 5 and 6.
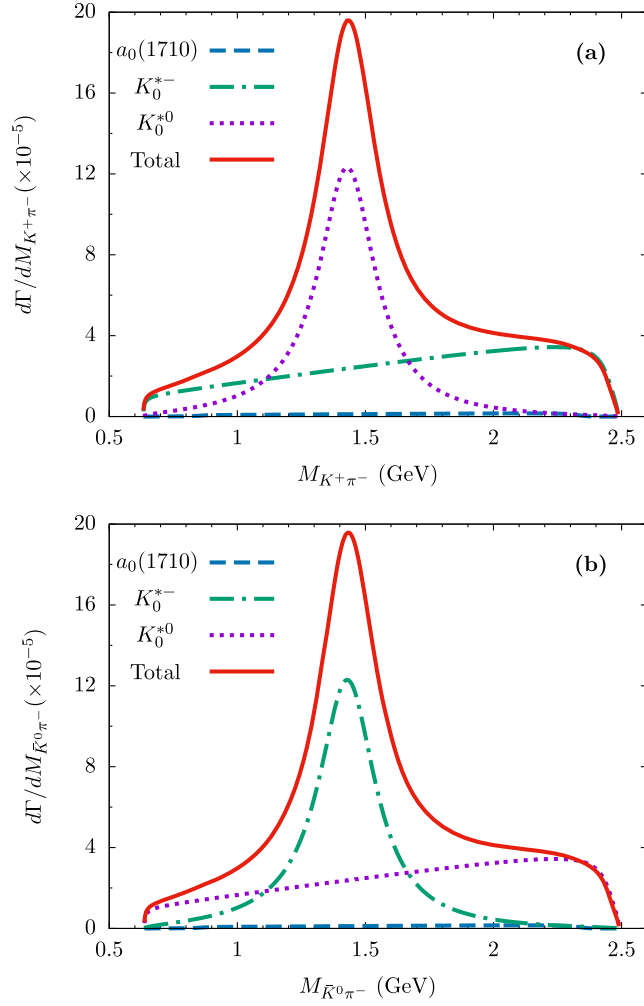
FIG. 8. $K^+\pi^-$ (a) and $\bar{K}^0\pi^-$ (b) invariant mass distribution of the process $\eta_c \to \bar{K}^0 K^+\pi^-$. The notations of the curves are the same as those of Fig. 5.

$\phi = 0$, $\pi/3$, $2\pi/3$, and π, we would obtain the $\bar{K}^0 K^+$ invariant mass distributions shown in Fig. 7, where one can see a peak structure around 1.8 GeV for $\phi = 2\pi/3$ and π.

Next, with the parameter $V_p = 0.8$, we predict the $K^+\pi^-$ and $\bar{K}^0\pi^-$ invariant mass distributions for the $\eta_c \to \bar{K}^0 K^+\pi^-$ in Figs. 8(a) and 8(b), respectively. One can see the clear peaks of the $K_0^*(1430)^0$ and $K_0^*(1430)^-$, which is consistent with the *BABAR* measurements [see Figs. 5(a) and 5(b) of Ref. [33]].

In Fig. 9, we present the Dalitz plots for the process $\eta_c \to \bar{K}^0 K^+\pi^-$ with the parameter $V_p = 0.8$. From Figs. 9(a) and 9(b), we can clearly see that there is a vertical blue band around $M_{\bar{K}^0 K^+} = 1.8$ GeV, which should be associated with the signal of the scalar $a_0(1710)$, and we also find a yellow band around $M_{\bar{K}^0\pi^-/K^+\pi^-} = 1.43$ GeV, corresponding to the signal of the $K_0^*(1430)$ state. From
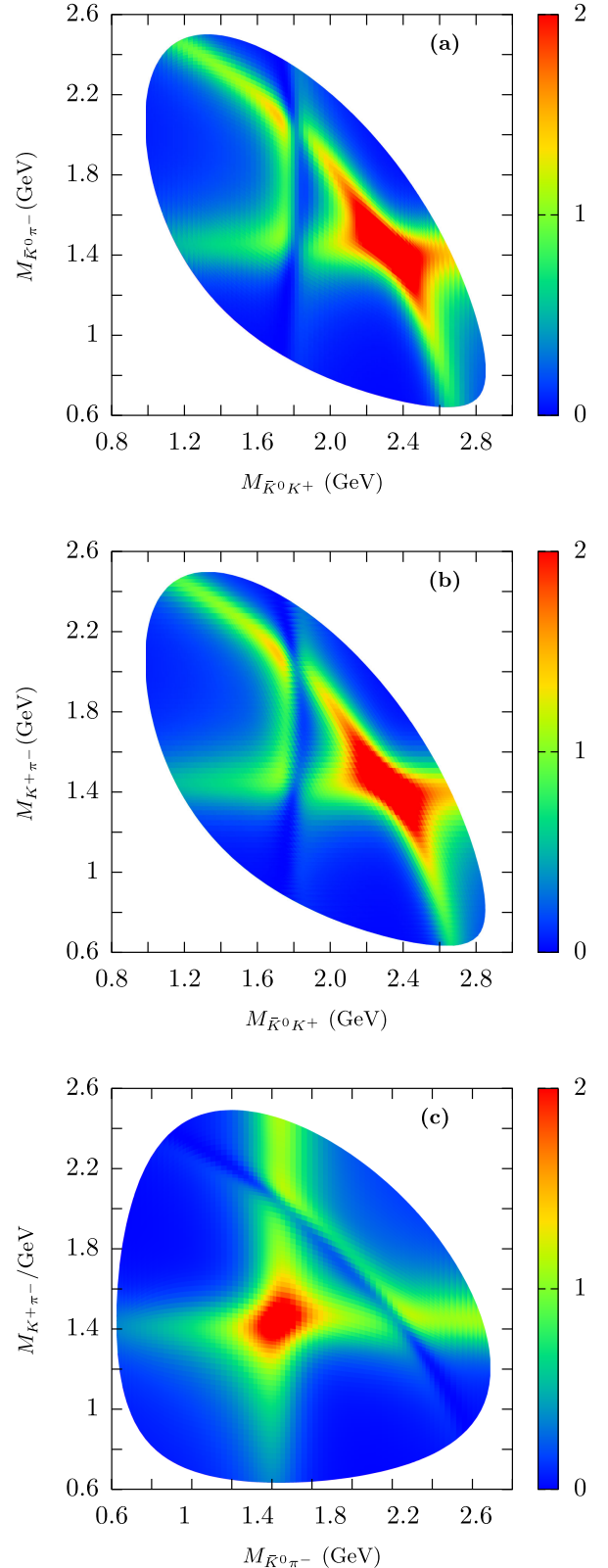
FIG. 9. Dalitz plots for the decay $\eta_c \to \bar{K}^0 K^+\pi^-$. (a) $M_{\bar{K}^0 K^+}$ vs $M_{\bar{K}^0\pi^-}$; (b) $M_{\bar{K}^0 K^+}$ vs $M_{K^+\pi^-}$; (c) $M_{\bar{K}^0\pi^-}$ vs $M_{K^+\pi^-}$.

Fig. 9(c), can see that most events of the process $\eta_c \to \bar{K}^0 K^+ \pi^-$ will appear in the region around $M_{\bar{K}^0 \pi^-} = 1.43$ GeV and $M_{K^+ \pi^-} = 1.43$ GeV, which is in agreement with the *BABAR* measurements (see Fig. 4 of Ref. [33]).

Finally, we predict the branching fractions of the processes $\eta_c \to \bar{K}^{*0} K^{*+} \pi^-$ and $\eta_c \to \omega \rho^+ \pi^-$, which have not yet been measured. Without the contributions from intermediate resonances, based on Eq. (3) the amplitudes for the processes $\eta_c \to \bar{K}^{*0} K^{*+} \pi^-$ and $\eta_c \to \omega \rho^+ \pi^-$ are,

$$\mathcal{M}^{\eta_c \to \bar{K}^{*0} K^{*+} \pi^-} = V_p \vec{\epsilon}_{\bar{K}^{*0}} \cdot \vec{\epsilon}_{K^{*+}}, \qquad (27)$$

$$\mathcal{M}^{\eta_c \to \omega \rho^+ \pi^-} = \sqrt{2} V_p \vec{\epsilon}_\omega \cdot \vec{\epsilon}_{\rho^+}, \qquad (28)$$

where $\vec{\epsilon}_i$ is the polarization of the vector meson, and $\sum_{\text{pol}} \epsilon_i(R) \epsilon_j^*(R) = \delta_{ij}$ [47]. With the parameter $V_p = 0.8$, we could estimate the branching fractions of these two processes,

$$\mathcal{B}(\eta_c \to \bar{K}^{*0} K^{*+} \pi^-) = \frac{1}{\Gamma_{\eta_c}} \int \left(\frac{d\Gamma}{dM_{\bar{K}^{*0} K^{*+}}} \right) dM_{\bar{K}^{*0} K^{*+}}$$
$$= 5.5 \times 10^{-3} \qquad (29)$$

$$\mathcal{B}(\eta_c \to \omega \rho^+ \pi^-) = \frac{1}{\Gamma_{\eta_c}} \int \left(\frac{d\Gamma}{dM_{\omega \rho^+}} \right) dM_{\omega \rho^+}$$
$$= 7.9 \times 10^{-3}, \qquad (30)$$

where the formalism of the differential width of the three-body decay could be found in the RPP [17]. We note that our prediction for $\mathcal{B}(\eta_c \to \bar{K}^{*0} K^{*+} \pi^-) = 5.5 \times 10^{-3}$ is less than $\mathcal{B}(\eta_c \to K^+ K^- \pi^+ \pi^- \pi^0) = (3.4 \pm 0.5)\%$ and $\mathcal{B}(\eta_c \to K^0 K^- \pi^+ \pi^- \pi^+) = (5.7 \pm 1.6)\%$, while the prediction for $\mathcal{B}(\eta_c \to \omega \rho^+ \pi^-) = 7.9 \times 10^{-3}$ is less than $\mathcal{B}(\eta_c \to 2(\pi^+ \pi^- \pi^0)) = (16.2 \pm 2.1)\%$ [17], which seem reasonable.

The BESIII Collaboration has collected 10 billion J/ψ events and 3 billion $\psi(3686)$ events, and the available η_c events via the decays of $J/\psi \to \gamma \eta_c$ and $\psi(3686) \to \gamma \eta_c$ are recently proposed to precisely measure the η_c decay modes [45], which could be helpful to search for the possible signal of the $a_0(1710)$, and test our theoretical predictions. The $\eta_c \to \bar{K}^0 K^+ \pi^-$ reaction could be a good platform to investigate the $a_0(1710)$, especially its mass.

It should be stressed that one can not exclude the other interpretations based the present experimental information. In Ref. [48], the authors have studied the coupled-channels influence on the $a_0(1710)$ line shape by assuming it as a

four-quark state in the MIT bag model, and found that the strong couplings of a_0 to VV channel can narrow the a_0 peak in the PP mass spectra, and the a_0 width could be 150–300 MeV in the absence of $K\bar{K}$ and $\pi \eta$ channels. It is suggested to detect the $a_0(1710) \to VV$ decay directly to test their results in Ref. [48].

IV. SUMMARY

Assuming the $a_0(1710)$ as a $K^* \bar{K}^*$ molecular state, we have investigated the process $\eta_c \to \bar{K}^0 K^+ \pi^-$ taking into account the contribution from the S-wave $\omega \rho^+$ and $\bar{K}^{*0} K^{*+}$ interactions, as well as the contribution from the intermediate resonance $K_0^*(1430)$. We predicted one dip structure around 1.8 GeV in the $\bar{K}^0 K^+$ invariant mass distribution, which is in agreement with the *BABAR* measurements [33]. It should be pointed out that a similar dip structure also appears around 1.8 GeV in the $K^+ K^-$ invariant mass distribution of the process $\eta_c \to K^+ K^- \pi^0$ of the *BABAR* measurements [46]. Furthermore, we predicted the $K^+ \pi^-$ and $\bar{K}^0 \pi^-$ invariant mass distributions of the process $\eta_c \to \bar{K}^0 K^+ \pi^-$, and found clear peaks of the resonance $K_0^*(1430)^{0,-}$, consistent with the *BABAR* measurements [33]. In addition, we have also plotted the Dalitz plots of the process $\eta_c \to \bar{K}^0 K^+ \pi^-$, and shown the possible signals of the $a_0(1710)$ and $K_0^*(1430)$.

Finally, we have estimated the branching fractions $\mathcal{B}(\eta_c \to \bar{K}^{*0} K^{*+} \pi^-) = 5.5 \times 10^{-3}$ and $\mathcal{B}(\eta_c \to \omega \rho^+ \pi^-) = 7.9 \times 10^{-3}$, which are reasonable by comparing with the experimental data. Our theoretical predictions could be tested by the BESIII and Belle II experiments in the future, and the precise measurements of the process $\eta_c \to \bar{K}^0 K^+ \pi^-$ could shed light on the nature of the scalar $a_0(1710)$.

ACKNOWLEDGMENTS

[1] J. P. Lees *et al.* (*BABAR* Collaboration), Phys. Rev. D **104,** 072002 (2021).

[2] M. Ablikim *et al.* (BESIII Collaboration), Phys. Rev. D **105,** L051103 (2022).

[3] M. Ablikim *et al.* (BESIII Collaboration), Phys. Rev. Lett. **129,** 182001 (2022).

[4] H. Nagahiro, L. Roca, E. Oset, and B. S. Zou, Phys. Rev. D **78,** 014012 (2008).

[5] T. Branz, L. S. Geng, and E. Oset, Phys. Rev. D **81,** 054037 (2010).

[6] L. S. Geng, F. K. Guo, C. Hanhart, R. Molina, E. Oset, and B. S. Zou, Eur. Phys. J. A **44,** 305 (2010).

[7] J. J. Xie and E. Oset, Phys. Rev. D **90,** 094006 (2014).

[8] A. Martinez Torres, K. P. Khemchandani, F. S. Navarra, M. Nielsen, and E. Oset, Phys. Lett. B **719,** 388 (2013).

[9] Z. L. Wang and B. S. Zou, Phys. Rev. D **104,** 114001 (2021).

[10] C. Garcia-Recio, L. S. Geng, J. Nieves, and L. L. Salcedo, Phys. Rev. D **83,** 016007 (2011).

[11] C. García-Recio, L. S. Geng, J. Nieves, L. L. Salcedo, E. Wang, and J. J. Xie, Phys. Rev. D **87,** 096006 (2013).

[12] F. E. Close and Q. Zhao, Phys. Rev. D **71,** 094022 (2005).

[13] L. C. Gui, Y. Chen, G. Li, C. Liu, Y.-B. Liu, J.-P. Ma, Y.-B. Yang, and J.-B. Zhang (CLQCD Collaboration), Phys. Rev. Lett. **110,** 021601 (2013).

[14] S. Janowski, F. Giacosa, and D. H. Rischke, Phys. Rev. D **90,** 114005 (2014).

[15] A. H. Fariborz, A. Azizi, and A. Asrar, Phys. Rev. D **92,** 113003 (2015).

[16] Y. Chen, A. Alexandru, S. J. Dong, T. Draper, I. Horvath, F. X. Lee, K. F. Liu, N. Mathur, C. Morningstar, M. Peardon *et al.*, Phys. Rev. D **73,** 014516 (2006).

[17] R. L. Workman *et al.* (Particle Data Group Collaboration), Prog. Theor. Exp. Phys. **2022,** 083C01 (2022).

[18] L. S. Geng and E. Oset, Phys. Rev. D **79,** 074009 (2009).

[19] M. L. Du, D. Gülmez, F. K. Guo, U. G. Meißner, and Q. Wang, Eur. Phys. J. C **78,** 988 (2018).

[20] Z. L. Wang and B. S. Zou, Eur. Phys. J. C **82,** 509 (2022).

[21] G. Y. Wang, S. C. Xue, G. N. Li, E. Wang, and D. M. Li, Phys. Rev. D **97,** 034030 (2018).

[22] D. Guo, W. Chen, H. X. Chen, X. Liu, and S. L. Zhu, Phys. Rev. D **105,** 114014 (2022).

[23] M. Ablikim *et al.* (BES Collaboration), Phys. Rev. Lett. **96,** 162002 (2006).

[24] M. Ablikim *et al.* (BESIII Collaboration), Phys. Rev. D **87,** 032008 (2013).

[25] X. Zhu, D. M. Li, E. Wang, L. S. Geng, and J. J. Xie, Phys. Rev. D **105,** 116010 (2022).

[26] X. Zhu, H. N. Wang, D. M. Li, E. Wang, L. S. Geng, and J. J. Xie, Phys. Rev. D **107,** 034001 (2023).

[27] L. R. Dai, E. Oset, and L. S. Geng, Eur. Phys. J. C **82,** 225 (2022).

[28] E. Oset, L. R. Dai, and L. S. Geng, Sci. Bull. **68,** 243 (2023).

[29] Z. Y. Wang, Y. W. Peng, J. Y. Yi, W. C. Luo, and C. W. Xiao, Phys. Rev. D **107,** 116018 (2023).

[30] X. Y. Wang, H. F. Zhou, and X. Liu, Phys. Rev. D **108,** 034015 (2023).

[31] M. Ablikim *et al.* (BESIII Collaboration), Phys. Rev. D **86,** 092009 (2012).

[32] M. Ablikim *et al.* (BESIII Collaboration), Phys. Rev. D **100,** 012003 (2019).

[33] J. P. Lees *et al.* (*BABAR* Collaboration), Phys. Rev. D **93,** 012005 (2016).

[34] J. P. Lees *et al.* (*BABAR* Collaboration), Phys. Rev. D **81,** 052010 (2010).

[35] N. Ikeno, J. M. Dias, W. H. Liang, and E. Oset, Phys. Rev. D **100,** 114011 (2019).

[36] S. J. Jiang, S. Sakai, W. H. Liang, and E. Oset, Phys. Lett. B **797,** 134831 (2019).

[37] H. Zhang, B. C. Ke, Y. Yu, and E. Wang, Chin. Phys. C **47,** 063101 (2023).

[38] J. Y. Wang, M. Y. Duan, G. Y. Wang, D. M. Li, L. J. Liu, and E. Wang, Phys. Lett. B **821,** 136617 (2021).

[39] M. Y. Duan, G. Y. Wang, E. Wang, D. M. Li, and D. Y. Chen, Phys. Rev. D **104,** 074030 (2021).

[40] A. Bramon, A. Grau, and G. Pancheri, Phys. Lett. B **283,** 416 (1992).

[41] R. Molina, D. Nicmorus, and E. Oset, Phys. Rev. D **78,** 114018 (2008).

[42] M. Y. Duan, D. Y. Chen, and E. Wang, Eur. Phys. J. C **82,** 968 (2022).

[43] L. S. Geng, E. Oset, R. Molina, and D. Nicmorus, Proc. Sci. EFT09 (**2009**) 040.

[44] G. J. Ding, Phys. Rev. D **79,** 014001 (2009).

[45] Q. Ji, S. Fang, and Z. Wang, arXiv:2108.13029.

[46] J. P. Lees *et al.* (*BABAR* Collaboration), Phys. Rev. D **89,** 112004 (2014).

[47] M. Y. Duan, E. Wang, and D. Y. Chen, arXiv:2305.09436.

[48] N. N. Achasov and G. N. Shestakov, Phys. Rev. D **108,** 036018 (2023).